Supporting Information for

ORIGINAL ARTICLE

Anti-PD-L1 antibody enhances curative effect of cryoablation *via* antibody-dependent cell-mediated cytotoxicity mediating PD-L1^{high}CD11b^{+} cells elimination in hepatocellular carcinoma

Jizhou Tan[a,b,†], Ting Liu[c,d,†], Wenzhe Fan[a,†], Jialiang Wei[a], Bowen Zhu[a], Yafang Liu[b], Lingwei Liu[a], Xiaokai Zhang[a], Songling Chen[b], Haibiao Lin[c,d], Yuanqing Zhang[e,*], Jiaping Li[a,*]

[a]*Department of Interventional Oncology, the First Affiliated Hospital, Sun Yat-sen University, Guangzhou 510080, China*

[b]*Department of Stomatology, the First Affiliated Hospital, Sun Yat-sen University, Guangzhou 510080, China*

[c]*Department of Laboratory Medicine, the Second Affiliated Hospital of Guangzhou University of Chinese Medicine, Guangdong Provincial Hospital of Traditional, Chinese Medicine, Guangzhou 510120, China*

[d]*Second Clinical Medical College, Guangzhou University of Chinese Medicine, Guangzhou 510006, China*

[e]*School of Pharmaceutical Sciences, Sun Yat-sen University, Guangzhou 510006, China*

Received 27 Mar 2022; received in revised form 15 June 2022; accepted 2 July 2022

***Corresponding authors.** Tel./fax: +86 20 87755766 (Jiaping Li).

E-mail addresses: zhangyq65@mail.sysu.edu.cn (Yuanqing Zhang), lijiap@mail.sysu.edu.cn (Jiaping Li).

†These authors made equal contributions to this work.

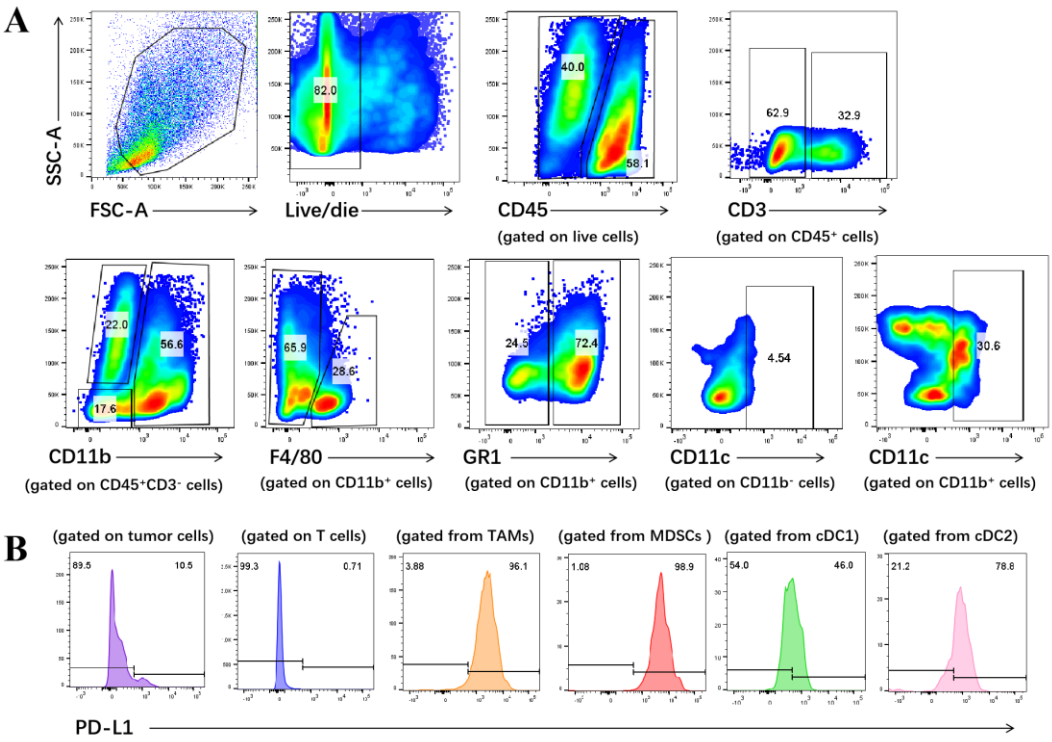

Figure S1. FACS gating strategy for Figure 1

Representative gating strategy was shown by flow cytometry analysis. Numbers in gates indicate the percentage of subsets. FACS gating strategy for analyzing the PD-L1^{+} phenotype on tumor cells, T cells and myeloid-drived immune cells in tumor microenvirnment.

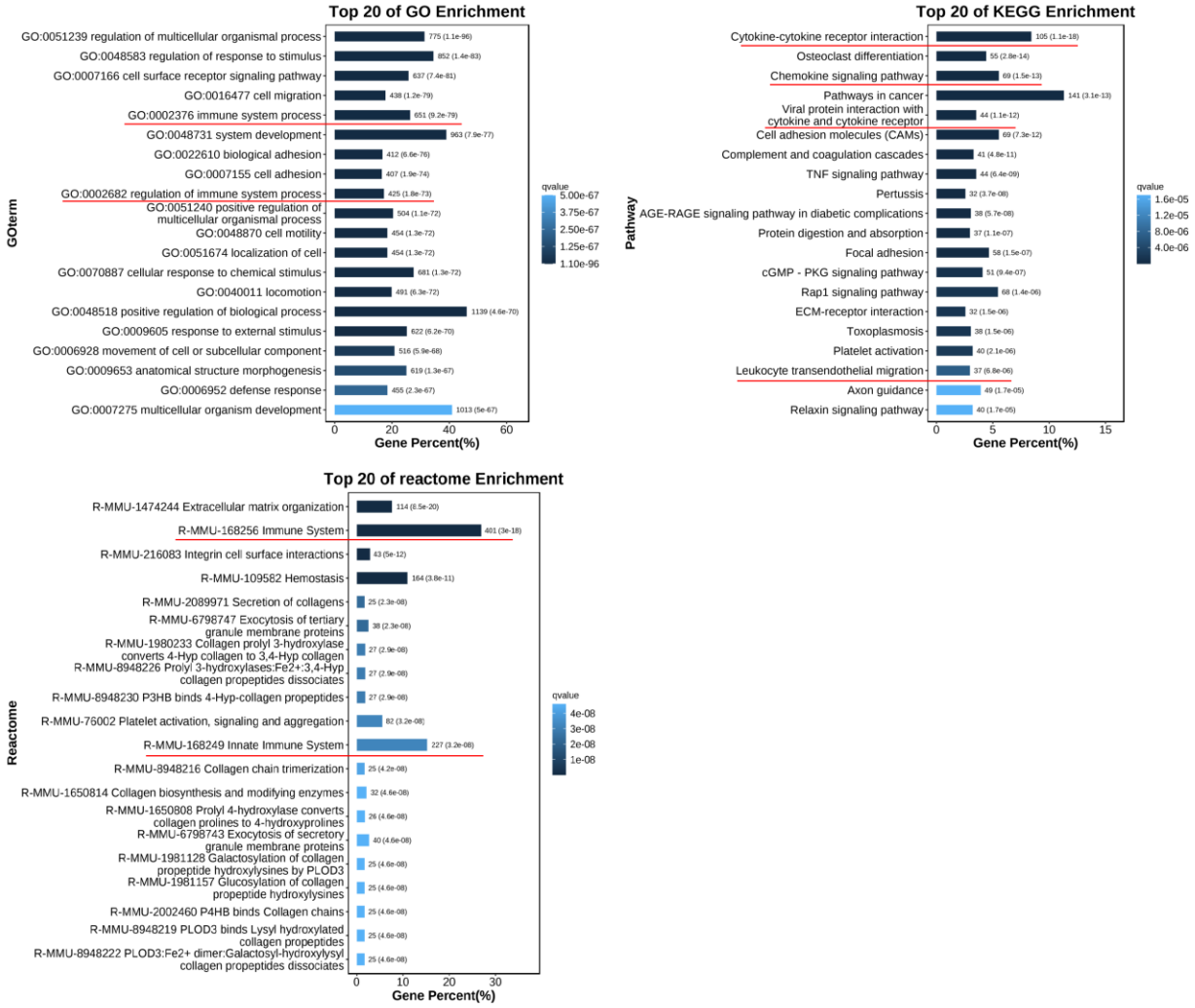

Figure S2. RNA-seq data of CD45$^+$ immune cells from cryoablation combined with anti-PD-L1 antibodies group (CAR+a-PDL1) compared with untreated group(NC).

GO enrichment, KEGG enrichment and Reactome enrichment demonstrated the significant enrichment of top 20 pathways using a P/Q value. Red underlines highlighted the pathways associated with immune responses.

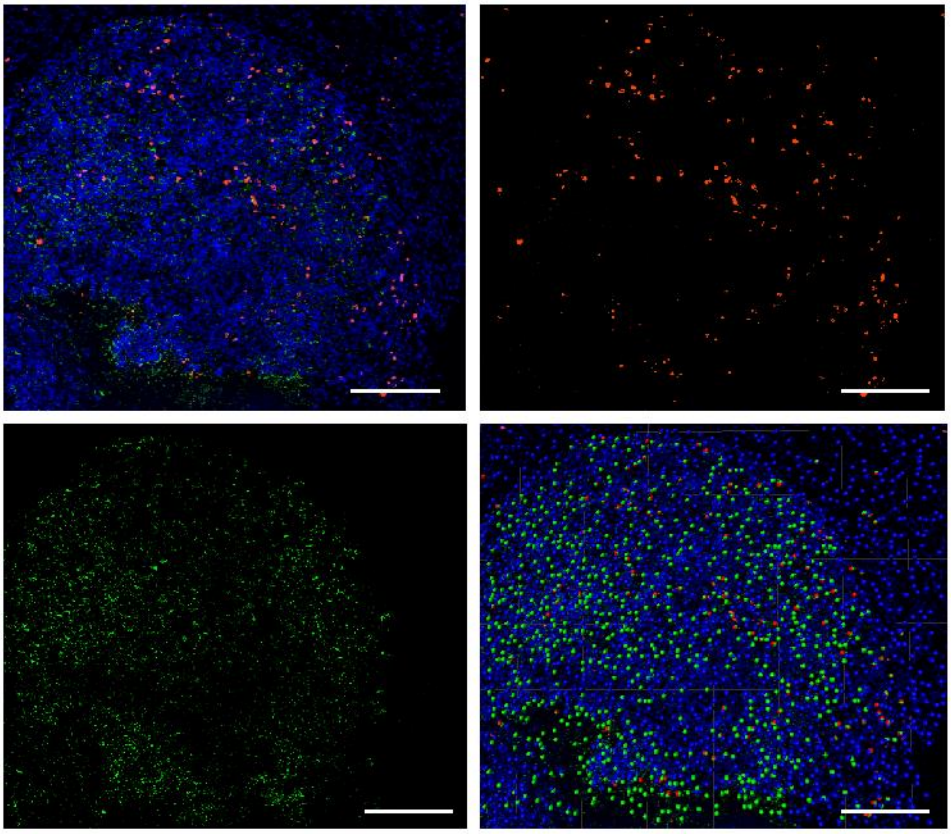

Figure S3. Example of quantification diagram of immunofluorescence views for immunofluorescence staining of tumor tissue sections.

Example immunofluorescence images. The Spot function of Imaris software located and enumerated $CD8^+$ T cells(red) , $CXCL9^+$ spots(green) and Dapi (blue) based on size and intensity threshold. Data was calculated by Imaris×64 V.7.4.2. Scale bar=200 μm.

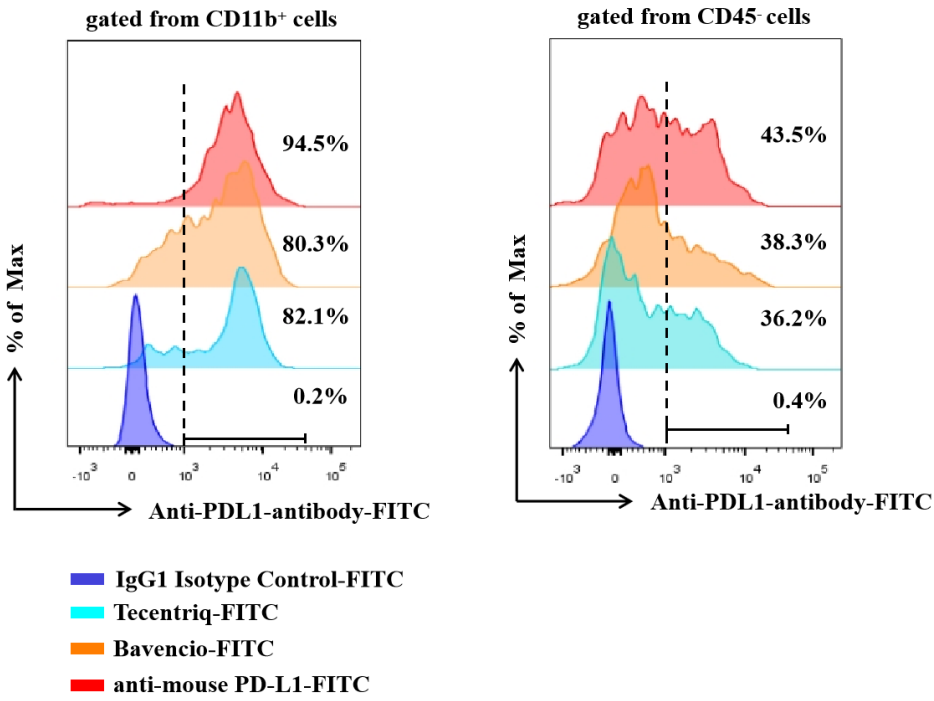

Figure S4. The affinity of two kinds of clinical anti-human PD-L1 antybodies to mouse CD11b$^+$ myeloid cells or tumor cells.

Tecentriq, Bavencio, human IgG1 isotype with N298A mutation (IgG1 Isotype control) and anti-mouse PD-L1 antibody (BE0033-2, BioXcell) were labeled with FITC fluorescence. The anti-mouse PD-L1 antibody was acted as a positive control. Antibodies were incubated with tumor cells or CD11b$^+$ cells isolated from mouse HCC models for 30 min. Flow cytometry analysis were used to test the affinity of different antibodies.

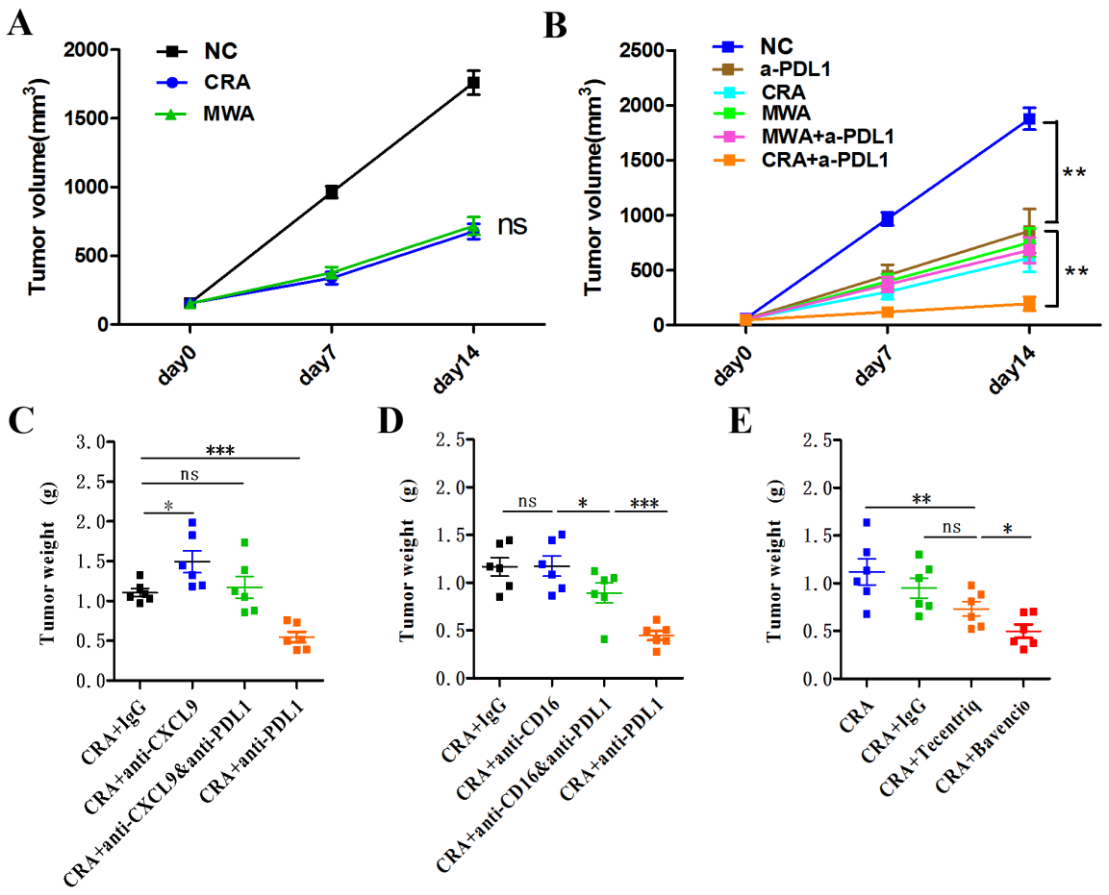

Figure S5 The tumor growth cure and the tumor weight at the end point of each animal experiment in corresponding Figures of main text.

(A, B) The tumor growth cure in Figure 1E (A), Figure 2C (B) of main text. (C, E) The tumor weight at end point in Figure 3L (C), Figure 5D (D), Figure 6G (E) of main text. *n*=6 for each groups, **P*<0.05, ***P*<0.01, ****P*<0.001. ns, no significant difference, t-tests. All data are means ± SEM.